JOURNAL OF MATERIALS SCIENCE 37 (2002) 1301 – 1308

Spectral analysis of transition metal-doped MgO "matched emitters" for thermophotovoltaic energy conversion

L. G. FERGUSON
Department of Materials Science and Engineering, University of Washington, Seattle, WA 98195, USA

F. DOGAN
University of Missouri-Rolla, Ceramic Engineering Department, Rolla, MO 65409, USA
E-mail: fdogan@u.washington.edu

A new, thermally excited Co/Ni-doped MgO ceramic emitter for TPV energy conversion is described in this work, and termed the "matched emitter" because its emissive power spectrum is very efficiently matched with the portion of the electromagnetic spectrum that can be converted directly into electrical energy by infrared responding GaSb photovoltaic cells. Ligand Field Theory calculations are used to estimate the crystal field splitting energies at high temperatures for Co and Ni-doped MgO matched emitters. Experimental measurements of the high temperature (1300–1400°C) emissive power spectrums for Co and Ni-doped MgO emitters are compared with predictions obtained from ligand field calculations for what is believed to be the first time. It was found that crystal field splitting energies of 10 Dq = 9070 cm^{-1} represented the "best fit" for the Co-doped MgO high temperature emissive power spectrum, and 10 Dq = 7950 cm^{-1} for the Ni-doped MgO spectrum. These values are only slightly lower than values reported for corresponding single crystal, transition metal doped laser materials that were measured at or well below room temperature.

1. Introduction

This paper will discuss theoretical and experimental aspects concerning recently developed, transition metal-doped selective emitters for thermophotovoltaic (TPV) energy conversion [1, 2]. The essential components for TPV energy conversion typically will include a low-bandgap, infrared-responding GaSb photovoltaic cell array in close proximity with a thermally excited radiant emitter element. Radiation from the high temperature emitter is converted to electricity when incident photons of sufficient energy are absorbed by the photovoltaic cell array. The radiant emitter element is heated to temperatures of about 1200°C–1400°C by the combustion of a hydrocarbon fuel such as methane or propane [3], GPHS radioisotope [4], or other heat source including concentrated sunlight (solar TPV) [5]. Research efforts have focused on the search for "spectrally selective" emitter materials with concentrated emissive power output at photon wavelengths that are most ideally "matched" to the response of the infrared photovoltaic cells.

TPV energy conversion can be highly efficient, clean, silent, and reliable given that TPV generators can be constructed with no moving parts, and the fact that infrared-responding photovoltaic cells are now capable of quantum yields that are greater than 90% when the range of incident photon energies is optimized [6]. Attempts to realize the advantages of TPV energy conversion, however, have met with only limited success. Some of the earliest experimental TPV generators used a combination of near "blackbody" or full-spectrum silicon carbide (SiC) emitters and silicon photovoltaic cells to convert radiation from the thermally excited emitter into electricity [7]. There are several problems that make this approach impractical. First, the bandgap energy of the Si photovoltaic cell is too large to convert energy with acceptable efficiency when the radiation source, or emitter, is at temperatures less than about 1700°C. Unfortunately, when the emitter must reach temperatures this high it is very difficult to find materials that maintain satisfactory spectral characteristics and have the ability to resist rapid deterioration, particularly when emitters are subjected to the strong oxidizing or reducing conditions that may be present during gas-fired generator operation. Another major problem has been the lack of any practical infrared filter that is capable of reflecting or recycling the large amount of non-convertible energy that is emitted by a full-spectrum, blackbody emitter material such as SiC. Any non-convertible radiation that is not reflected back and re-absorbed by the emitter will drastically lower the conversion efficiency of the system, and result in a destructive heat load on the temperature-sensitive photovoltaic cells and other generator components.

Some of the earliest work on spectrally selective emitters for TPV energy conversion involved the identification and high temperature characterization of several rare-earth oxides, particularly erbium oxide and ytterbium oxide [8]. These rare-earth oxides were shown to have emissive power peaks that were at near optimal wavelengths for photovoltaic energy conversion with Ge or Si cells, however the narrow "line-type" emissions did not give the improvement in spectral efficiency that researchers had hoped for.

With few exceptions, nearly all of the prior research on spectrally selective emitters has centered on rare earth oxide-based materials, and methods to improve the convertible power density. Researchers at the Space Power Institute, for example, have developed a "Multiple-Dopant Selective Emitter" [9]. Their approach includes using carefully chosen mixtures of holmia, erbia, and other rare earth oxides in an effort to maximize the number of characteristic emissive power peaks that occur within the optimal wavelength range for photovoltaic conversion. Unfortunately, the holmia emissions (around 2.01 μm) are outside of the conversion range for the simpler, low-cost GaSb photovoltaic cells, and more complex ternary InGaAs, or quaternary GaInAsSb photovoltaic cells are required to take advantage of the increased spectral power density.

The novel emitters that will be described in this work have the critical advantage of not emitting energy at non-convertible wavelengths in the first place. The new Co/Ni-doped MgO emitters are termed "matched emitters" because their spectral emissivity is selective, and can be concentrated at wavelengths where the quantum yield of infrared-responding GaSb photovoltaic cells is highly efficient [10]. By the same principle, the matched emitters also emit very little energy at non-convertible wavelengths, so that the problems of energy recycling and thermal loading are reduced to a manageable level.

The distribution of radiant energy is controlled and optimized in the matched emitter by introducing Co/Ni transition-metal dopant ions that are spectrally active within a low emissivity MgO host lattice. The matched emitters are similar to solid-state laser materials, (Cr_2O_3 doped Al_2O_3 ruby laser for example) in that emissions are the result of intra-atomic electronic transitions that are determined by the electronic configuration of the dopant ions and interactions with the coordinating crystal field of the host oxide [11].

2. Experimental procedure and discussion

The matched emitter materials were fabricated by tape casting methods from slurries containing doped MgO powders and binders, (a detailed description can be found in [1]). Flexible tapes were cut as ribbons (approx. 125 μm thick and 2 mm wide) and woven to construct flat panels. After sintering at 1520°C, the panels made from the woven ribbons are strong enough to withstand the pressure of hot combustion gasses impinging on them, and yet not too massive to prevent excellent heat transfer or thermal coupling with the hot gas combustion products.

Emissive power measurements at temperatures of 1200–1500°C are required to characterize and evaluate potential emitter materials. A multifunction spectral measurement station was constructed for the purpose of making high-quality measurements of materials and components that are intended for use in TPV generators. Emitter materials, in the form of single ribbons or panels, are held in a rigid fixture and heated to temperatures of about 1200–1500°C by using an air-propane gas flame to make the emissive power measurement.

A wavelength of about 1.7 μm corresponds to the minimum energy photon that is required to promote electrons to the conduction band in an infrared-responding GaSb photovoltaic cell. In previous works [1, 2, 10] it has been shown that NiO-doped MgO emitters radiate almost as much power as a theoretical blackbody within the convertible wavelength range between about 1 and 1.7 μm, while emissive power outside of this "useful" range is greatly suppressed due to the novel chemistry of the transition-metal doped MgO matched emitter. Dopant (or Co/Ni impurity ion concentrations) of about 1 to 2 mol% are preferred because these levels appear to represent an optimal tradeoff between nearest neighbor interactions and peak spectral density. If the dopant concentration is decreased below the optimal range, then spectral emissive power in the convertible wavelength range decreases towards the minimal levels of the undoped MgO host. If the dopant concentration is increased much above the optimal level, then nearest neighbor Co/Ni interactions begin to dominate and there is a rapid increase in spectral emissive power at non-convertible wavelengths that degrades the spectral selectivity and efficiency of the matched emitter [10]. Among the refractory oxides that may be used as emitter host materials, magnesium oxide has emerged as a superior material because it has the best combination of infrared transparency at long wavelengths and excellent chemical stability of the Co/Ni dopants at high temperatures.

When compared to full-spectrum blackbody emitters under similar test conditions, it is found that the transition-metal doped MgO emitters require much less fuel or thermal input energy to generate an equivalent amount of electrical power in a standard GaSb photovoltaic cell. This result is easily understood in terms of an energy balance. Far less thermal input energy is needed to balance the total power being radiated away by the spectrally selective, transition-metal doped MgO matched emitter when compared with the full-spectrum blackbody emitter.

The "ideal" radiant emitter for use with GaSb photovoltaic cells would have an emissive power spectrum with maximum radiant power between about 1.0 μm and 1.7 μm, and minimal output at other wavelengths. The experimental measurements included in Figs 4 and 6 show that the spectral emissive power of the "bandgap matched" transition-metal doped MgO emitters described in this work closely approximate this ideal power spectrum for energy conversion with GaSb photovoltaic cells.

3. Charge transfer and bandgap theory

Multiple theories have been advanced to explain the interactions between matter and radiation, and the

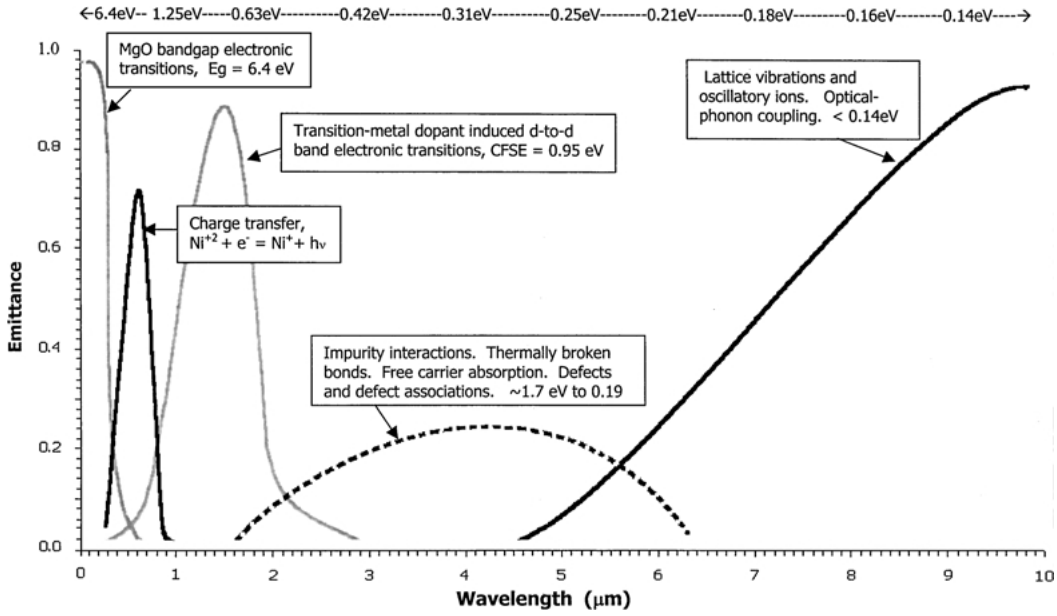

Figure 1 Emittance for a generalized "matched emitter" showing spectral components with probable radiation mechanisms.

characteristic spectral behavior that results. These include ionic models, energy band models, crystal field and ligand field theories, molecular orbital theory, and intermediate theories. No single theory appears to adequately describe the entire radiation spectrum of transition-metal doped selective emitters, and various theories will therefore be used in this work to interpret different portions of the measured spectrums.

Fig. 1 is a conceptual spectrum that is meant to show each of the underlying component radiation mechanisms that contribute to the high temperature spectral emittance that is characteristic of transition-metal doped MgO "matched emitters". It should be said that the assignment of radiation mechanisms is somewhat speculative, and the transition region between "spectral components" is not usually abrupt or precisely identified.

The region of high emittance beginning at about 200 nm and extending to shorter wavelengths in Fig. 1 can be explained in terms of radiative electronic transitions across an energy bandgap that is intrinsic to MgO. A highly stoichiometric, ionic solid such as pure MgO may be classified as a closed-shell insulator because each Mg atom donates 2 electrons from its outer $3s^2$ orbitals to create a closed $2p^6$ shell around the O atom. An energy bandgap is created between a filled band having bonding orbitals with predominately oxygen $2p$ character, and an empty 'metal cation' band of anti-bonding orbitals. The room temperature electronic energy band gap for MgO is reported to be about 7.65 eV [12]. According to experimental measurements by French [13], the bandgap decreases with increasing temperature at a rate of about -1.0 meV/K. The effective intrinsic bandgap at an emitter operating temperature of 1427°C would therefore be about 6.25 eV. This would imply strong optical absorption beginning around 198 nm where incident photons would have enough energy to promote an electron from the valence band up into the conduction band. The correspondence principle between absorption and emission tells us that energetic electrons in the upper conduction band would also emit photons at similar energies (wavelengths < 200 nm) as they drop down into the valence band.

Before turning to focus on the spectral contributions of extrinsic defects in the MgO, some comments on the far infrared spectral component in Fig. 1 should be made. It is evident that there is a monotonic increase in the emittance that begins at about 5 μm and approaches the theoretical maximum around 9 or 10 μm. A comparison between intentionally doped and "nearly pure" MgO emitters suggests that the far infrared spectral component is nearly independent of both the doping levels and temperature. It can be concluded that the radiant emissions in this range depend primarily on an intrinsic property of the host MgO material (within the present doping range and operating temperatures at least). Insulators, such as MgO, are believed to have a light absorption mechanism caused by light induced vibrations of the lattice atoms, or excitation of phonons by photons. Diatomic solids exhibit mechanical resonances based on the masses of the two ion species, and the restoring forces (or binding strength) that the ions experience in the crystal lattice. The phonons take the form of traveling waves and may interact to produce photons in the quantum mechanical scheme. The high emittance in this long-wavelength region around 9 μm (characteristic of most ceramic oxides) is of interest because the most efficient emitter materials for TPV applications will be host ceramic oxides that minimize all non-convertible radiation at wavelengths longer than about 1.7 μm. A simple diatomic linear lattice model and calculations (described in more detail elsewhere [14]) show that the infrared absorption edge moves towards longer wavelengths when the mass of the constituent ions is increased or the effective ionic charge is reduced, and when the bonding energy is weaker or the lattice separation is increased there is the opposite effect.

The focus will change now to the spectral contributions of *extrinsic* defects in the MgO based emitter, including the intentional dopants (CoO and NiO), as well as other impurities that may be unintentional.

Quantifying the effects of extrinsic defects in the MgO-based emitter will be a primary objective because these intentional defects provide the radiative transitions resulting in high spectral efficiency for TPV applications. The radiant emissions that can most likely be connected with charge transfer processes are first estimated from energy band theory, and then detailed interband d-d transitions are compared with the results of ligand field theory calculations.

Charge transfer transitions involve the loss of an electron to the conduction band, the capture of an electron from the valence band, or the transfer of an electron to another species (charge exchange). The precise positions of localized energy levels within the fundamental bandgap of an insulator such as MgO are difficult to calculate, and the results will only be suitable for qualitative charge transfer estimates.

A particularly significant disadvantage of the local density formalism is that electron repulsion terms that determine the energies of different crystal field states are not correctly calculated [15]. This problem can be partly compensated by calculating different orbitals for different spins. This is the approach taken by Timmer and Borstel [16] in their calculation of the electronic structure of substitutional Co^{+n}, Ni^{+n}, and Fe^{+n} impurities in the MgO host lattice.

An energy level diagram and calculations from the above work by Timmer and Borstel [16] are reproduced here in Fig. 2. The energy levels of each localized state that resulted from the substitution of a Ni^{+n} ion for an Mg^{+2} ion were measured with respect to the valence and conduction bands, according to the scale on the vertical axis. Labels for probable charge transfer transitions, as well as conventional electron spin configurations have been added by the authors to the original Figure by Timmer and Borstel [16] for the purposes of discussion. According to molecular orbital theory, the oxygen 2p orbitals and the metal d^n orbitals combine to form the t_{2g} and e_g levels shown in Fig. 2. The t_{2g} orbitals are filled with 6 electrons and the e_g levels are filled with 4 electrons. The ground state configuration for a d^8 Ni^{+2} ion in octahedral coordination is the $t_{2g}^6 e_g^2$ *configuration*, and this particular configuration is called the $^3A_g^2$ *state*. (Note that symmetry term symbols such as 3A, 3F, 1D, and 3P, should not be confused with the 4s, 4p, and 3d-type energy levels of the free ions.) The octahedral crystal field of the 6 surrounding oxygen ions splits the t_{2g} and e_g levels, and this difference is called the crystal field splitting energy (CFSE). The CSFE is about equal to 1.05 eV for a substitutional Ni^{+2} ion in the MgO host crystal. The orbital energies for spin-down electrons are higher than for spin-up electrons, and as a consequence the energy levels for spin-down electrons are shown to be higher than for spin-up electrons. The calculated t_{2g} and e_g energy levels are different for the Ni^{+1}, Ni^{+2}, and Ni^{+3} valency states. The valency states with one empty e_g orbital are lower in energy than those with no empty e_g orbitals because stronger mixing takes place with the excited charge transfer configurations. If the thermal energy k_bT is lower than the CFSE then low-spin configurations will be formed (electrons in the upper e_g levels are unpaired). At an operating temperature of 1700 K the thermal energy k_bT is about 0.14 eV, and is therefore definitely less than the CFSE = 1.05 eV for Ni^{+2} ions in the MgO lattice, resulting in the unpaired (parallel) spin configurations in Fig. 2.

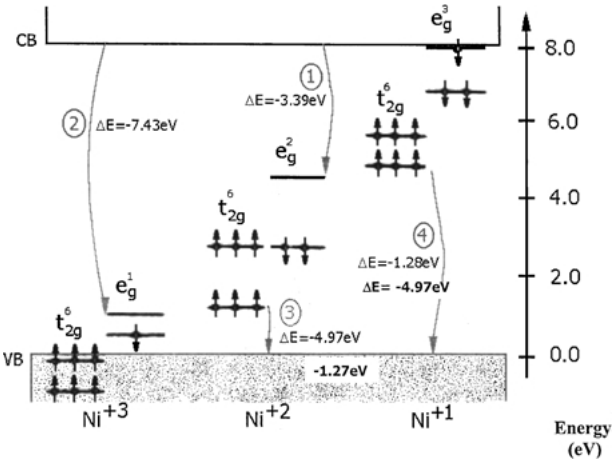

Figure 2 Positions of localized energy levels for Ni^{+n} ions within host MgO bandgap. (Calculated by Timmer and Borstel [16]).

TABLE I Charge transfer in Ni-doped MgO

1.	$Ni^{+2} + e^- \rightarrow Ni^{+1} + h\nu$	Acceptor	$\Delta E = -3.39$ eV
2.	$Ni^{+3} + e^- \rightarrow Ni^{+2} + h\nu$	Acceptor	$\Delta E = -7.43$ eV
3.	$Ni^{+2} - e^- \rightarrow Ni^{+3} + h\nu$	Donor	$\Delta E = -1.28$ eV
4.	$Ni^{+1} - e^- \rightarrow Ni^{+2} + h\nu$	Donor	$\Delta E = -4.97$ eV

The electronic charge transitions that can be associated with the emission of photons are identified in Fig. 2, and labeled accordingly in Table I,

Several researchers have attempted to make charge transfer identifications based on spectroscopic absorption data [17–20]. Because of all the complications, the number of unambiguously assigned charge transfer energies is rather small, as Cox [15] has observed. In one article, Blazey [17] concluded that the charge transfer process from the O^{-2} ligand to Ni^{+2} impurities in MgO has an absorption threshold of about 6.2 eV at impurity concentrations of 850 ppm, and that the intensity increases with Ni-dopant concentration. According to Fig. 2, the charge transfer process taking an electron from the O^{-2} valence states to the empty e_g low-spin orbital for the Ni^{+2} ion would be,

$$Ni^{+2} + e^- \rightarrow Ni^{+1} + h\nu \qquad \text{Acceptor-type}$$
$$\Delta E = +4.62\,\text{eV}$$

where Ni^{+1} is by convention the acceptor charge state *after* gaining an electron. The measured value of $\Delta E = +6.2$ eV (if correctly assigned by Blazey [17]) is significantly different than the theoretical value above. This type of discrepancy appears to be not unusual for the charge transfer calculation.

Cox [15] has stated that the Franck-Condon principle might be used to explain these discrepancies and has noted that spectroscopic transitions are expected to be different from the fully relaxed thermal transitions. The calculated transitions are intended to predict thermodynamic stability, and include slow atomic relaxation terms that do not play a role in the purely electronic

process. Thermal activation energies are about 1–2 eV less than optical energies according to estimates, and this would make for much better agreement between the measured charge transfer energies and those calculated in Fig. 2. In light of this argument, it certainly seems reasonable to regard the charge transfer energies as determined in Fig. 2 as minimum values, and this has important consequences for the TPV application. The lowest energy charge transfer transition (labeled #3 on Fig. 2) is expected to generate photons with energy of at least 1.28 eV. This means that all charge transfer contributions to the emissive power spectrum for Ni-doped MgO would have to be at wavelengths less than about 950 nm, and outside of the 1 to 1.7 μm range that is most efficient for photovoltaic energy conversion with low-bandgap GaSb photovoltaic cells.

4. Interband, d-d orbital transitions and ligand field calculations

The interband d-d orbital transitions for Ni-doped MgO are discussed in the context of ligand field theory in this section. According to Nassau [11], the transition elements having unpaired electrons in their d or f orbitals can absorb light by ligand field controlled transitions that do not involve variable valence states.

Tetrahedrally coordinated $CoCl_2$ is known to be blue in the anhydrous state, yet in the octahedrally coordinated hydrated form, $CoCl_2 \cdot 6H_2O$, is pink. The fact that magnesium oxide also turns a distinctive "pink" color when it contains a small percentage of cobalt suggests that the surrounding oxygen atoms octahedrally coordinate the cobalt ions. The molecules or atoms that surround the cobalt ion produce an electrostatic field called the crystal field or ligand field. The symmetry and the strength of the ligand field are controlling factors in determining the electronic transitions that are responsible for absorption and radiation of light when coordination compounds involve transition metal ions, such as Co^{+2} or Ni^{+2}, with incompletely filled outer d-orbitals.

When coordinating ligands surround an ion, the electronic orbital energies of that ion may be raised to higher levels if the ligand field is symmetrical with respect to the orbitals of the ion. The six oxygen atoms that surround the Mg^{+2} ion in MgO, for example, create an octahedrally symmetric coordinating ligand field. The Mg^{+2} ion also has octahedrally symmetric p-type orbitals in its outer electron shell, and this raises the energy of those orbitals and creates a large forbidden energy gap (about 7.8 eV). The substitution of an antisymmetrical ion, Co^{+2} or Ni^{+2} for example, having partially filled d-orbitals in its outer shell causes splitting of the d-orbitals (that were previously energetically equivalent) and the creation of new interband energy levels.

Some insight can be gained by contrasting the 3d transition-metals with the spectroscopic behavior of rare-earth ions such as erbia or ytterbia that have radiant emissions originating in the deeper lying, partially-filled 4f orbitals. In the case of the rare-earth ions, the unfilled shells involve deep-lying 4f electrons that are well shielded by the completely filled $5s^2 5p^6$ orbitals. The energy levels of the *free* rare-earth ion are essentially unchanged when the free ion is embedded in a solid, unlike the 3d transition-metal ion where the energy levels are profoundly changed [21]. The radiant emissions from the rare-earth ions consist of narrower "lines" that resemble the emissions of the free ion, whereas the emissions from the 3d transition metal ions originate from multiple new energy levels and form much broader "bands". It is evident that the radiant emissions of the 3d transition metal ions are then largely dictated by the symmetry of the field due to the surrounding ions, and can be "spectrally engineered" to a greater degree than the rare-earth selective emitters by altering the dopants or impurities within the oxide host.

Term Diagrams have been calculated by Tanabe and Sugano [22] showing how available energy levels vary with the crystal field parameter, "Dq", for the most commonly occurring octahedral and tetrahedral coordinating ligand configurations. When a Co^{+2} ion substitutes for an Mg atom in MgO, the Co^{+2} ion enters into a site of octahedral symmetry with an electronic orbital occupation of $3d^7$. In the absence of an external crystal field, the d-orbitals of a transition metal atom would all have different orientations, but the same energy. As a result of the antisymmetrical, metal ion-octahedral crystal field interactions, the energy equality of the five d-orbitals is destroyed, and instead the 3d orbitals split into two higher (the e_g orbitals) and three lower (the t_{2g} orbitals) energy configurations. The term symbols, such as $^4T_1$ and $^4T_2$, give the overall symmetry behavior with the net spin $(2S+1)$ in the superscript. The electron configuration for octahedrally coordinated Co^{+2} in the ground state, $^4T_1(F)$, is $(t_{2g}^2 e_g^5)$.

According to the spin selection rule, $\Delta S = 0$, the octahedral Co^{+2} configuration is predicted to have three spin allowed transitions to the ground state, $^4T_2(F) \rightarrow {}^4T_1(F)$, $^4A_2(F) \rightarrow {}^4T_1(F)$, and $^4T_1(P) \rightarrow {}^4T1(F)$, that will correspond to strong emissions and absorption. The intermediate transition, $^4A_2(F) \rightarrow {}^2E(G)$, is believed to be responsible for strong infrared emissions at 1487 nm. Although this intermediate transition does not strictly obey the spin selection rules, there is a high probability that energetic electrons decay from nearby higher energy levels such as the $^2T_2(G)$ level by non-radiative phonon-coupled processes involving lattice vibrations. The transition from $^4A_2(F)$ to $^2E(G)$ must be completed by the emission of a photon because the energy gap is too large for decay by non-radiative processes. In this particular case ($3d^7$ Co^{+2} ion in octahedral coordination), the energy difference for the lowest transition, $^4T_2(F) \rightarrow {}^4T_1(G)$, is defined as the crystal field splitting energy, 10 Dq. There are nine different d-orbital occupation schemes for transition metals with octahedral coordinating ligands, and the same number of corresponding Term Diagrams [22].

When a Co^{+2} ion substitutes for an Mg atom in MgO, the Co^{+2} ion enters into a site of octahedral symmetry with an electronic orbital occupation of $3d^7$. The appropriate energy level diagram for a $3d^7$ substitutional ion in octahedral symmetry was obtained from a paper by Low [23], and this diagram was used to construct Fig. 3. The vertical line, labeled $Dq = 907\ cm^{-1}$ in Fig. 3, is the crystal field parameter for the cobalt-doped MgO matched emitter that gave the "best fit"

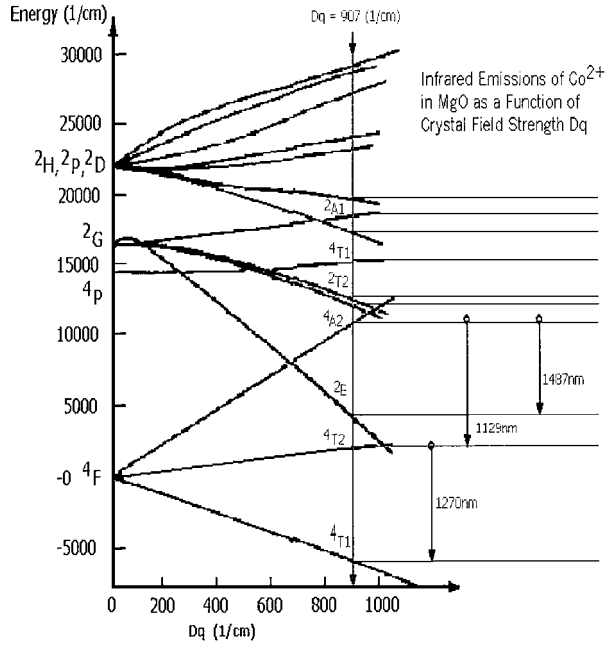

Figure 3 Energy level diagram for Co^{+2} ($3d^7$) ion in octahedral coordination at a temperature of about 1300–1400°C. The vertical line labeled $Dq = 907\ cm^{-1}$ gives the "best-fit" between the crystal field parameter, Dq, and energy level transitions corresponding to the emissive power peaks for the 2 wt% Co_3O_4-doped MgO matched emitter ribbon shown in Fig. 4.

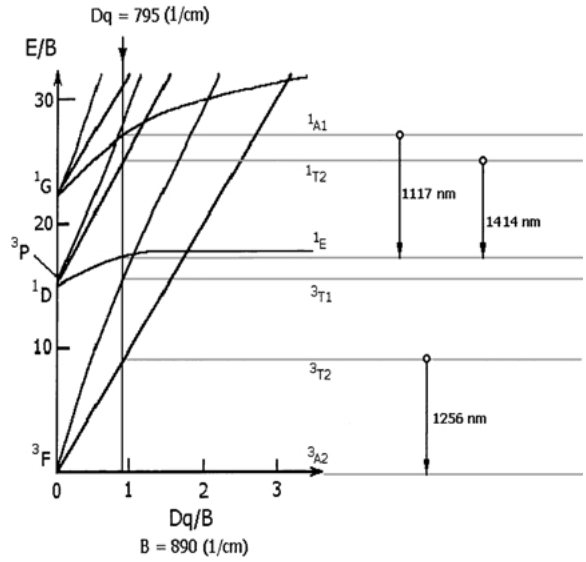

Figure 5 Energy level diagram for a Ni^{+2} ($3d^8$) substitutional ion in octahedral symmetry at a temperature of about 1300–1400°C. The vertical line labeled $Dq = 795\ cm^{-1}$ gives the "best-fit" between the crystal field parameter, Dq, and energy level transitions corresponding to the emissive power peaks for the 4 wt% NiO-doped MgO matched emitter ribbon shown in Fig. 6.

with respect to measurements of the high-temperature emissive power spectrum for that emitter. The "best fit" was accomplished by the repetitive task of estimating a trial value for Dq, drawing a vertical line, and then making high-resolution graphical measurements of the distance on the energy scale between allowable transitions. The discrete energies of radiative transitions obtained from the energy level diagram were then converted to wavelengths ($\lambda = hc/\Delta E$) and superimposed on the measured emissive power spectrum. This process was repeated until a close correspondence between the major allowed energy level transitions and the structure of the peaks in the emissive power spectrum was obtained, and the results are shown in Fig. 4. Only the major infrared transitions, such as $^4T_2(F) \rightarrow {}^4T_1(F)$, are labeled.

When a Ni^{+2} ion substitutes for an Mg^{+2} ion in MgO, the Term Diagram for a $3d^8$ substitutional ion in octahedral symmetry must be used. An appropriate $3d^8$ Term Diagram was found in a text by Figgis [24] and used to construct Fig. 5, in a manner similar to the case for Co-doped MgO. A value of $Dq = 795\ cm^{-1}$ gave the "best fit" for the high-temperature, Ni-doped MgO emissive power spectrum. The wavelengths of three major radiative energy transitions, $^3T_2 \rightarrow {}^3A_2$,

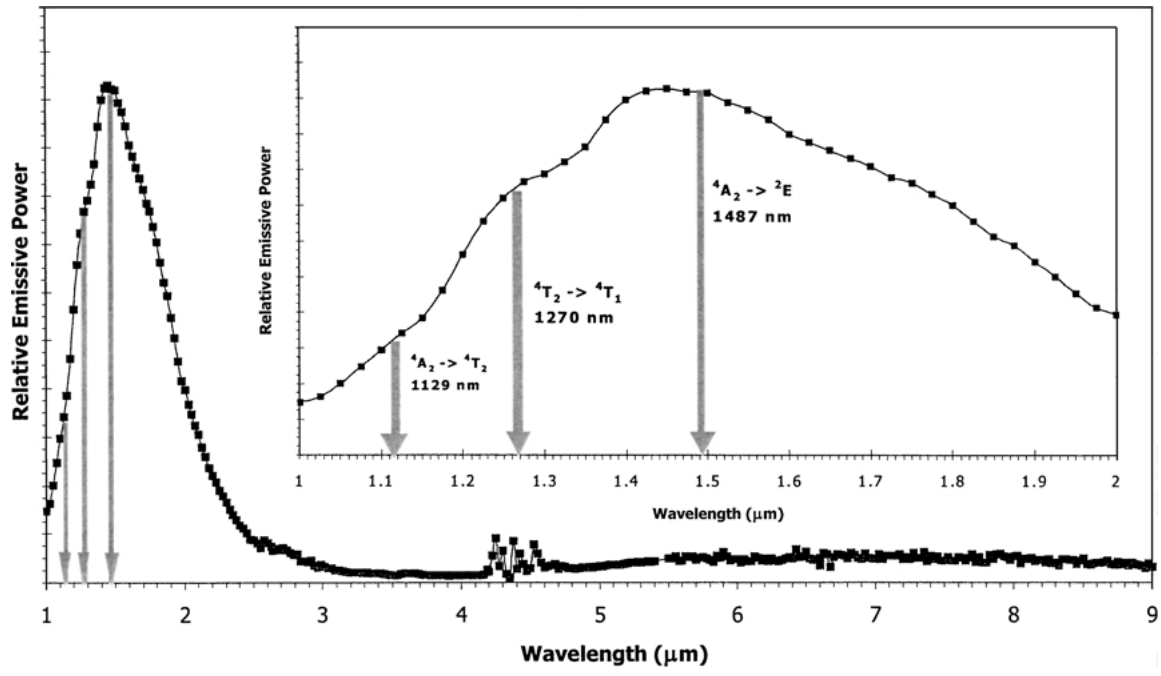

Figure 4 Emissive power spectrum for a 2 wt% Co_3O_4-doped MgO tapecast ribbon at a temperature of about 1300–1400°C, and corresponding radiative transitions from Fig. 3 for Co^{+3} ($3d^7$) ion in octahedral symmetry.

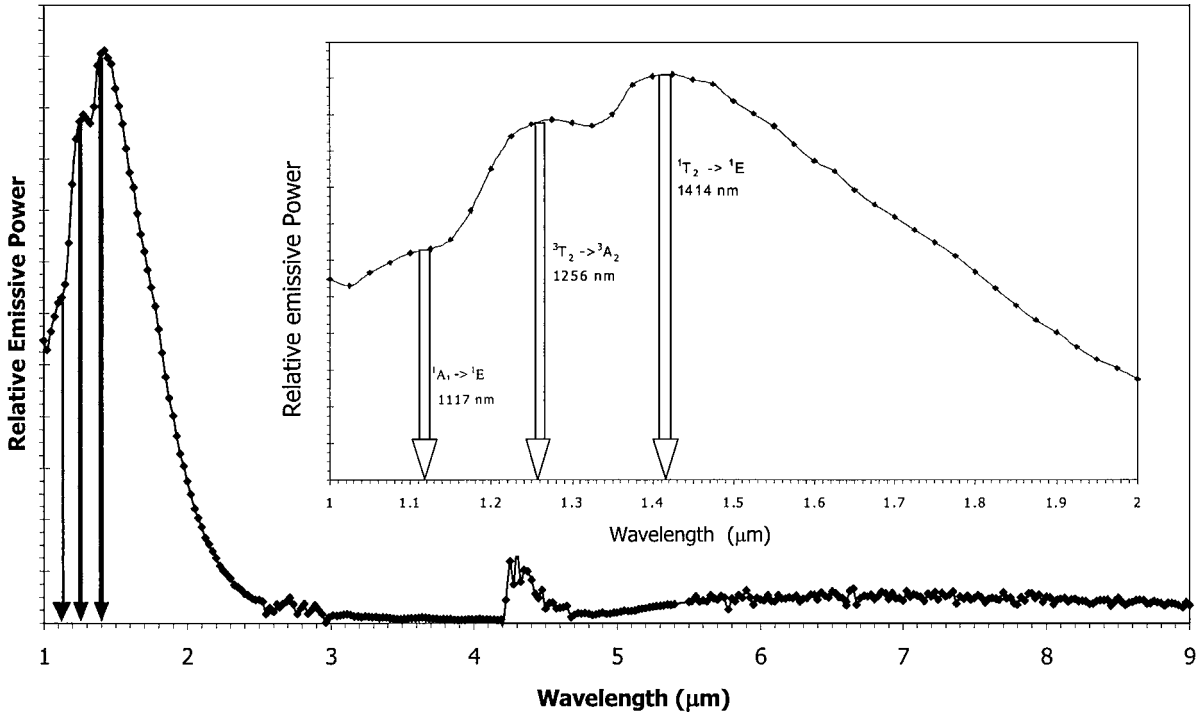

Figure 6 Emissive power spectrum for a 4 wt% NiO-doped MgO tapecast ribbon at about 1300–1400°C and corresponding radiative transitions from Fig. 5 for Ni^{+2} ($3d^8$) ion in octahedral symmetry.

$^1T_2 \rightarrow {}^1E$, $^1A_1 \rightarrow {}^1E$, and the measured emissive power spectrum are shown in Fig. 6.

Values of crystal field strength, Dq, for a variety of transition metal-doped laser materials appear in the published literature. Although these published values for Dq are nearly always measured at liquid nitrogen temperatures, the preliminary results presented in this work indicate that they can be useful for predicting the emissive power spectrums of transition metal-doped MgO matched emitters at much higher temperatures.

The absorption and emission spectrums for single crystal, transition metal-doped MgO have been measured by several researchers at temperatures of 77 K, where much more spectral detail can be resolved. Because of lattice vibrations and the associated modulation of Dq the radiative transitions between energy levels are broadened at higher temperatures, and discrete emission peaks smear into bands. Most of the previous interest in transition-metal ion doped MgO has centered on low-temperature broadband or tunable laser applications (no data for temperature greater than 300°K could be found in the literature.) Low [23] made absorption measurements at room temperature and 77 K, and obtained a Dq of 960 cm^{-1} for Co-doped MgO. Pappalardo [25] made more extensive absorption measurements at 78 K and 4.2 K and obtained a Dq of 927 cm^{-1}. The value of 927 cm^{-1} for Dq at a temperature of 78 K is probably the most reliable. It appears that the crystal field splitting energy obtained at very high temperatures, $Dq = 907\ cm^{-1}$, is only slightly weaker than the crystal field at 78 K.

Reports [26–29] concerning both the optical absorption spectrum, and emission spectrum, of $3d^8(Ni^{2+})$ in MgO have appeared in the literature. The reported values for Dq and temperatures are summarized in Table II.

TABLE II Crystal field splitting energies, 10 Dq, for $3d^8(Ni^{+2})$ in MgO

10 Dq (cm^{-1})	Temperature (K)	Reference
8600	298	Low [26], 1958
8150	78	Pappalardo [27], 1961
8763	79	Bird [28], 1972
8310	80	Moncorge' [29], 1988

The discrepancies in Table II are not easily explained. Bird [28] claims to have made a "complete" Ligand Field calculation, but their value for Dq is significantly higher than more recent measurements by Moncorge' [29]. The value of $10\ Dq = 8150\ cm^{-1}$ at 78 K that was reported by Pappalardo [27] appears to be very consistent now with the "best fit" value of $10\ Dq = 7950\ cm^{-1}$ that was obtained for the high-temperature Ni-doped MgO ribbon emitter. The shift in crystal field energy is 200 cm^{-1}, and is exactly the same as the Co-doped MgO ribbon emitter.

5. Conclusions

A new thermally excited emitter material for TPV energy conversion has been described in this work and termed the "matched emitter" because its emissive power spectrum is very efficiently matched with the portion of the spectrum that can be converted into electrical energy by infrared responding photovoltaic cells. It has been shown that doping concentrations of 1 to 2 mol% Co_3O_4 or NiO within a low infrared emissivity MgO host will produce matched emitters with continuous, strong radiant emissions in the optimal energy range between approximately 1 and 1.9 μm, and minimal radiation at non-convertible wavelengths.

Experimental measurements have shown that power densities of almost 9 W/cm^2, in the convertible wavelength range between 1 and 1.9 μm, and temperatures of 1400°C or more are easily achieved with NiO-doped MgO tape cast emitters in an air-propane flame with no energy recycling (IR filters). Power densities of only 2 W/cm^2 are considered suitable for many important applications such as satellite, terrestrial remote power, and the co-generation of heat and power for military and commercial users. A power density of 9–10 W/cm^2 may be adequate for some of the most demanding applications, such as powering an electric vehicle.

Ligand Field Theory calculations and the measured emissive power spectrums for Co and Ni-doped MgO matched emitters have been used to estimate the crystal field splitting energies at high temperatures. It was found that 10 Dq = 9070 cm^{-1} represented the "best fit" for the Co-doped MgO high temperature emissive power spectrum, and 10 Dq = 7950 cm^{-1} for the Ni-doped MgO spectrum. These values are only slightly lower than values reported for corresponding single crystal, transition metal doped laser materials that were measured at or well below room temperature.

Acknowledgements

We would like to acknowledge grants and support from the Washington Technology Center, and JX Crystals, Inc., of Issaquah Washington. We would also like to thank Dr. Thomas G. Stoebe for helpful discussions.

References

1. L. G. FERGUSON and F. DOGAN, *J. Mater. Sci.* **36** (2001) 137.
2. *Idem.*, *Materials Science and Engineering* B **83** (2001) 35.
3. T. J. COUTTS, *Renewable and Sustainable Energy Reviews* **3** (1999) 77.
4. A. SCHOCK and V. KUMAR, in 1st NREL, Conference on Thermophotovoltaic Generation of Electricity, AIP Conf. Proc. 321, Copper Mountain, CO, 1994, edited by T. J. Coutts and J. P. Benner (American Institute of Physics, 1995) p. 139.
5. D. L. CHUBB, B. S. GOOD and R. A. LOWE, in 2nd NREL Conference on Thermophotovoltaic Generation of Electricity, AIP Conf. Proc. 358, Colorado Springs, CO, 1995, edited by J. P. Benner, T. J. Coutts, D. S. Ginley (American Institute of Physics, 1996) p. 181.
6. SUNDARAM, S. B. SABAN, M. D. MORGAN, W. E. HORNE, B. D. EVANS, J. R. KETTERL, M. B. Z. MOROSINI, N. B. PATEL and H. FIELD, in 3rd NREL Conference on Thermophotovoltaic Generation of Electricity, AIP Conf. Proc. 401, Colorado Springs, CO, 1997, edited by T. J. Coutts, C. S. Allman and J. P. Benner (American Institute of Physics, 1997) p. 105.
7. E. KITTL, in Proc. 20th Annual Power Sources Conference (PSC Publ. Comm., Red Bank, NJ, May 1966) p. 178.
8. G. E. GUAZZONI, *Applied Spectroscopy* **26** (1972) 60.
9. Z. CHEN, P. L. ADAIR and M. F. ROSE, in 3rd NREL Conference on Thermophotovoltaic Generation of Electricity, AIP Conf. Proc. 401, Colorado Springs, CO, 1997, edited by J. P. Benner, T. J. Coutts and D. S. Ginley (American Institute of Physics, 1997) p. 181.
10. L. G. FERGUSON, Ph.D. Dissertation, Department of Materials Science and Engineering, University of Washington, March 2000.
11. K. NASSAU, "The Physics and Chemistry of Color—The Fifteen Causes of Color" (Wiley, New York, 1983).
12. Y.-M. CHIANG, D. P. BIRNIE III and W. D. KINGERY, "Physical Ceramics" (John Wiley and Sons, 1997).
13. R. H. FRENCH, *J. Amer. Ceram. Soc.* **73** (1990) 477.
14. L. L. HENCH and J. K. WEST, "Principles of Electronic Ceramics" (Johns Wiley and Sons, New York, 1990).
15. P. A. COX, "Transition Metal Oxides" (Oxford Science Publications, 1992).
16. G. TIMMER and G. BORSTEL, *Physical Review* B **43** (1991) 5098.
17. K. W. BLAZEY, *Physica* **89B** (1977) 47.
18. A. M. STONEHAM and M. J. SANGSTER, *Phil. Mag.* B **43** (1981) 609.
19. K. W. BLAZEY, *J. Phys. Chem. Solids* **38** (1977) 671.
20. M. KUNZ and C. KLINGSSHIRN, *Materials Chemistry and Physics* **25** (1990) 27.
21. G. R. FOWELS, "Introduction to Modern Optics" (Holt, Reinehart and Winston, New York, NY, 1975).
22. Y. TANABE and S. SUGANO, *J. Phys. Soc. Japan* **9** (1954) 753, 766.
23. W. LOW, *Physical Review* **109** (1958) 256.
24. B. N. FIGGIS, "Introduction to Ligand Fields" (Wiley, New York, NY, 1966).
25. R. PAPPALARDO, D. L. WOOD and R. C. LINARES, JR., *The Journal of Chemical Physics* **35** (1961) 2041.
26. W. LOW, *Physical Review* **109** (1958) 247.
27. R. PAPPALARDO, D. L. WOOD and R. C. LINARES, JR., *The Journal of Chemical Physics* **35** (1961) 1460.
28. B. D. BIRD, G. A. OSBORNE and P. J. STEPHENS, *Physical Review* B **5** (1972) 1800.
29. R. MONCORGE' and T. BENYATTOU, *Physical Review* B **37** (1988) 9186.

Received 4 June
and accepted 29 November 2001